Supporting Information

Wrinkled Micropillar Surfaces Inspired by Moss Leaves for Ultrafast Superspreading and Cooling

Guoliang Liu[a,b], Jianning Yu[a,b], Haitao Deng[a,b], Zhongpeng Zhu[c], and Ye Tian[*a,b,c]

a Laboratory of Bio-inspired Smart Interface Science, Technical Institute of Physics and Chemistry, Chinese Academy of Sciences, Beijing 100190, China.

b University of Chinese Academy of Sciences, Beijing 100049, China.

c School of Nano Science and Technology, Suzhou Institute for Advanced Research, University of Science and Technology of China, Suzhou 215123, China.

* Corresponding author. E-mail: tianyely@iccas.ac.cn

This PDF file includes:

Supplementary Figures

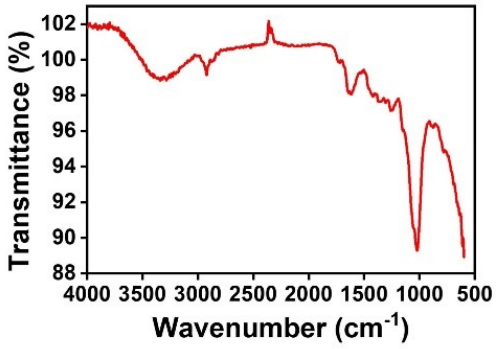

Figure S1. FTIR-ATR characterization of the leaves of *R. canescens*. The mainly surface composition of dried leaves of *R. canescens* is cellulose.

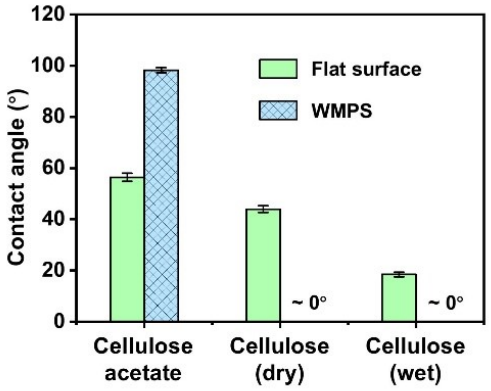

Figure S2. Contact angles of flat surfaces and WMPSs before and after hydrolysis. *Cellulose acetate* represents the sample without alkaline hydrolysis treatment. *Cellulose (dry)* represents the sample after alkaline hydrolysis, followed by oven-drying at 60°C for 1 h to remove moisture. *Cellulose (wet)* represents the hydrolyzed sample stored in water, with only surface moisture blown off before measurement.

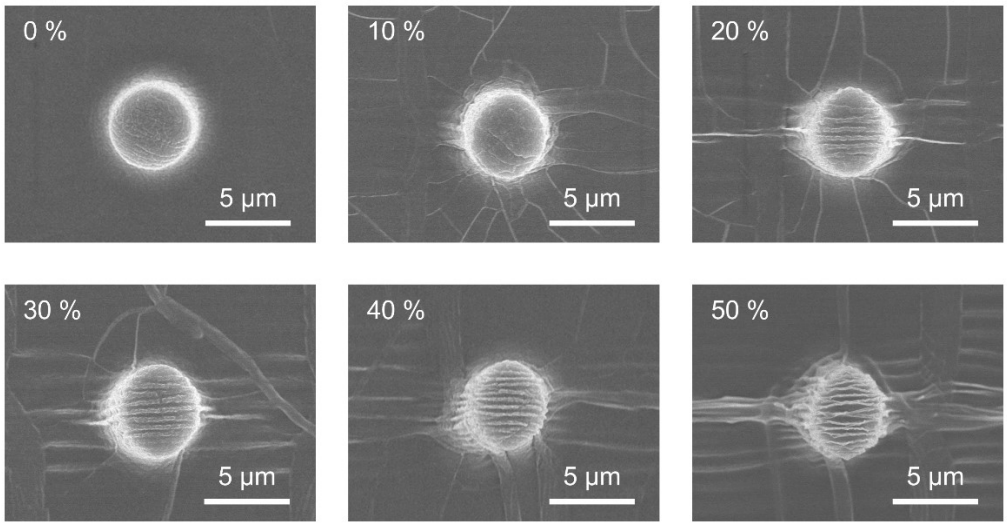

Figure S3. Representative SEM images of WMPS prepared with pre-stretching strains $\varepsilon = 0$, 10%, 20%, 30%, 40%, and 50%.

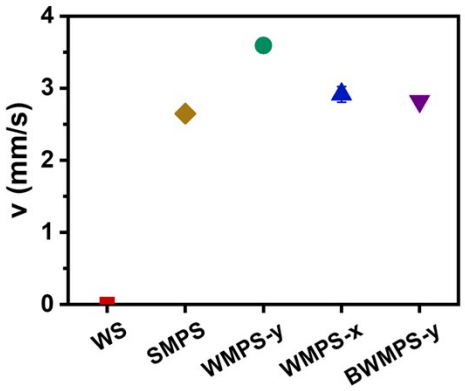

Figure S4. Variation in spreading velocity on different surfaces. WS refers to the wrinkled surfaces without micropillar arrays. The superspreading process is enabled by the hydrophilic micropillar array, while the wrinkles accelerate this process.

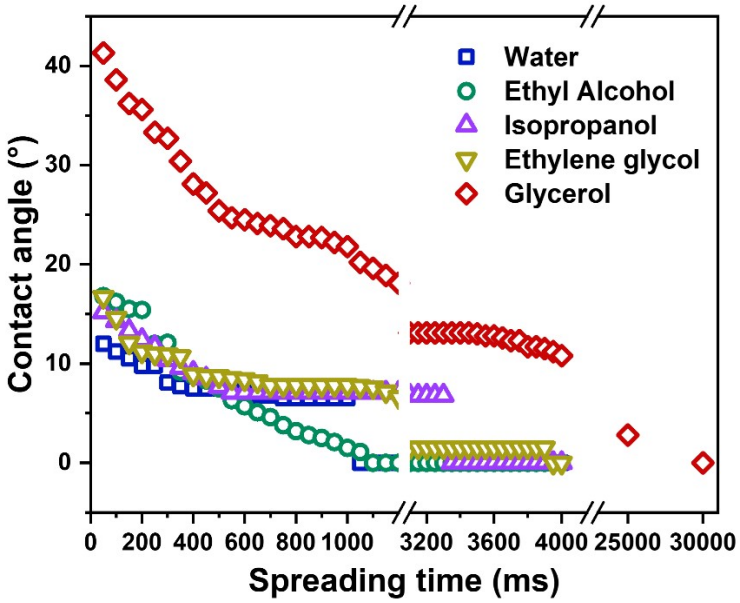

Figure S5. Spreading kinetics of different liquids on WMPS.

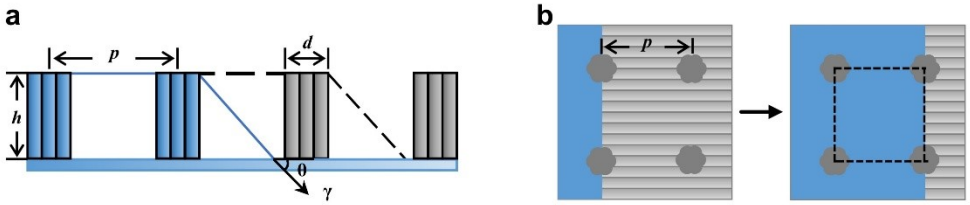

Figure S6. Theoretical model for dynamic water spreading on WMPS. (a) Side view of the microscopic spreading process. (b) Top view of the microscopic spreading process. The dashed-line box defines a structural unit, which is a square with side length *p*.

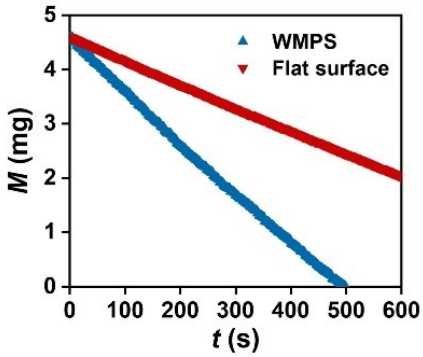

Figure S7. Weight loss curves of water in dark environment.

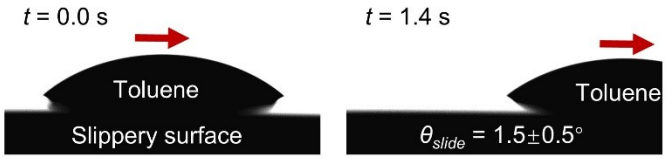

Figure S8. The water film on the wet-state WMPS creates a slippery interface, enabling oil droplets to slide off.

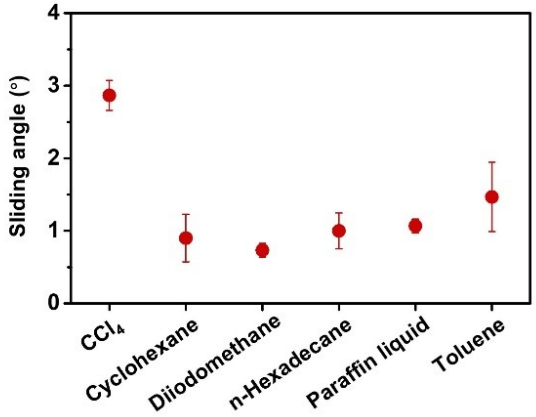

Figure S9. Roll-off angles of various oil droplets on the slippery WMPS surface.

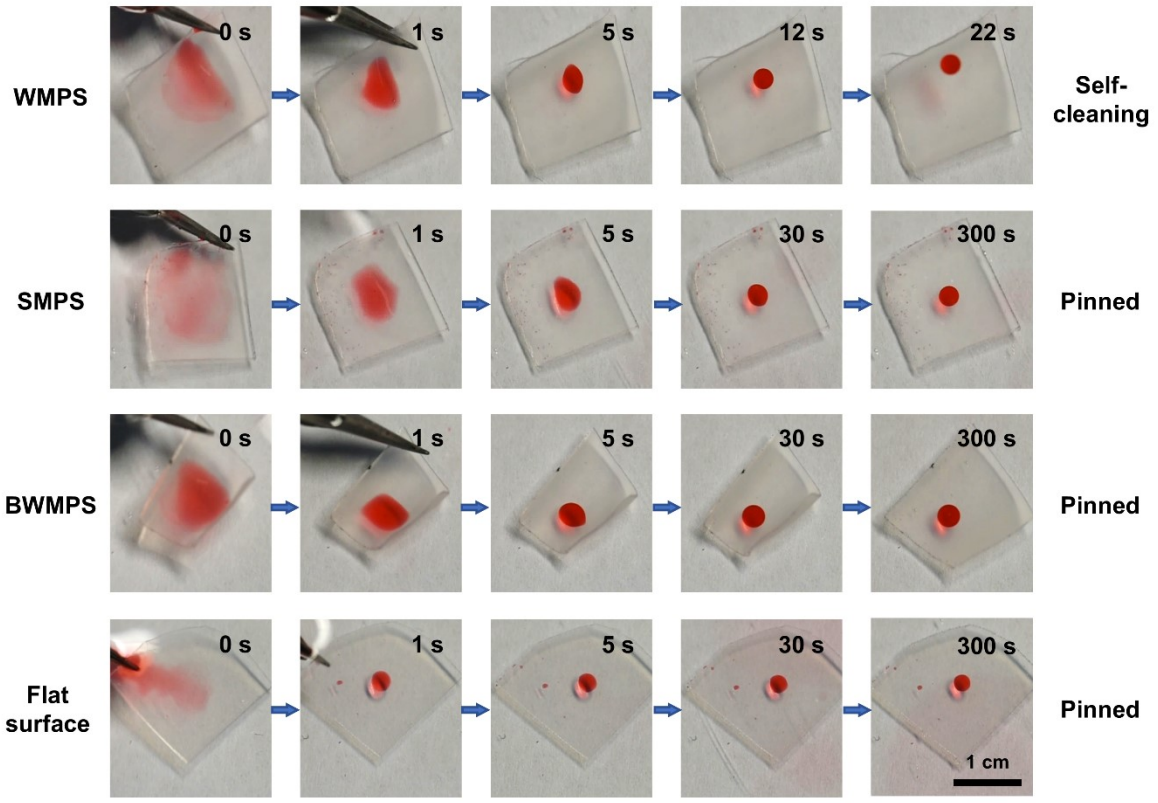

Figure S10. Demonstration of the self-cleaning capability of the WMPS against oil droplets. After immersion in water, the oil droplet on the WMPS dewets and detaches spontaneously, whereas on other structured surfaces, the droplet ultimately remains pinned.

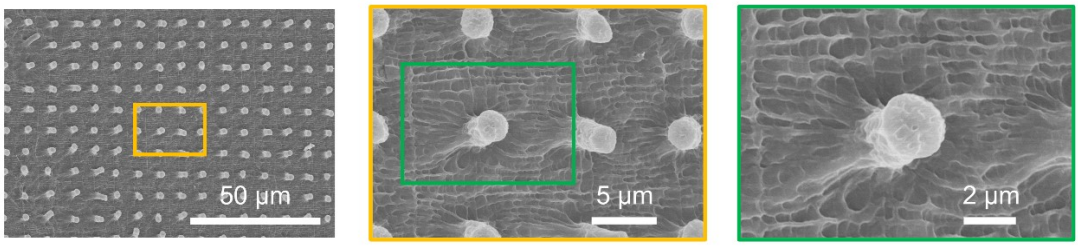

Figure S11. SEM image of the WMPS fabricated using PVA hydrogel as the casting material.

Comparison of water dynamic spreading on WMPS and SMPS.

We first consider dynamic spreading in the SMPS, that is, smooth micropillar array arranged inside the square lattice.[1] The roughness (r) occupied by the pillars is expressed as

$$r = 1 + \frac{\pi dh}{p^2} \tag{S1}$$

where d, h and p represent the diameter, the height and the pitch of micropillars, respectively.

The volume fraction of the solids (φ_s) is expressed as

$$\varphi_s = \frac{\pi d^2}{4p^2} \approx 0.09 \tag{S2}$$

The evolution of the front can be derived from the Onsager principle.[2] Assuming the wetted area has a length L and a width W, the free energy of the system is expressed as

$$E = \gamma\, LW[(1 - \varphi_s) - (r - \varphi_s)\cos\theta] \tag{S3}$$

where γ is the surface tension of the liquid and θ is the intrinsic contact angle of the substrate material.

Substitute Equation (S1) and Equation (S2) into Equation (S3), the free energy of the system is expressed as

$$E \approx -\pi dh\,\gamma\cos\theta\,\frac{LW}{p^2} \tag{S4}$$

The change rate of the free energy is expressed as

$$\dot{E} = -\pi dh\,\gamma\cos\theta\,\frac{W}{p^2}\dot{L} \tag{S5}$$

The resistance during liquid spreading on micropillar-arrayed surfaces originates from two distinct mechanisms: micropillar-induced shear resistance and substrate interfacial resistance. For a square array of cylinder, the frictional force on one cylinder is expressed as

$$F_r = hf(\varphi_s)\mu v \tag{S6}$$

where $f(\varphi_s)$ is a numerical factor.[3] For $\varphi_s = 0.09$, $f(\varphi_s) \approx 25$. The dissipation Φ_r caused by micropillar-induced shear resistance is expressed as

$$\Phi_r = \frac{1}{2} h f(\varphi_s) \mu \dot{L}^2 \frac{LW}{p^2} \tag{S7}$$

The substrate resistance per structural unit, derived from Newtonian shear stress formulation $\tau = \mu(\partial u/\partial y)$, is expressed as

$$F_b = \frac{\mu v (4p^2 - \pi d^2)}{4h} \tag{S8}$$

The dissipation Φ_b caused by substrate interfacial resistance is expressed as

$$\Phi_b = \frac{1\mu(4p^2 - \pi d^2)}{8 \quad hp^2} \dot{L}^2 LW \tag{S9}$$

The evolution of the dynamic spreading front is given by $\mathrm{d}/\mathrm{d}L(\dot{E} + \Phi) = 0$. This leads to

$$L\dot{L} = \frac{4\pi d h^2 \gamma \cos\theta}{\mu\left[4h^2 f(\varphi_s) + 4p^2 - \pi d^2\right]} \tag{S10}$$

The front propagation follows the standard Lucas-Washburn scaling

$$L_i = \sqrt{\frac{8\pi d h^2 \gamma \cos\theta}{\mu\left[4h^2 f(\varphi_s) + 4p^2 - \pi d^2\right]} t} \tag{S11}$$

where L_i is the dynamic spreading distance in the micropillar array.

Then, we take the surface wrinkles into consideration. We assume the WMPS surface has uniform sinusoidal wrinkles, where the arc length S in one wrinkle period λ satisfies the geometric constraint

$$S = n\lambda \ (n > 1) \tag{S12}$$

The roughness (r') occupied by the pillars and wrinkled is expressed as

$$r' = n + \frac{n\pi d h}{p^2} \tag{S13}$$

The volume fraction of the solids ($\varphi_s{}'$) is considered to remain unchanged

$$\varphi_s{}' \approx \varphi_s = \frac{\pi d^2}{4p^2} \tag{S14}$$

the free energy of the system is expressed as

$$E' \approx - n\pi dh\,\gamma \cos\theta \frac{LW}{p^2} \tag{S15}$$

The change rate of the free energy is expressed as

$$\dot{E}' = - n\pi dh\,\gamma \cos\theta \frac{W}{p^2}\dot{L} \tag{S16}$$

The dissipation $\Phi_r{}'$ caused by wrinkled-micropillar-induced shear resistance is expressed as

$$\Phi_r{}' = \frac{1}{2} nhf(\varphi_s)\mu\,\dot{L}^2 \frac{LW}{p^2} \tag{S17}$$

The dissipation $\Phi_b{}'$ caused by wrinkled-substrate interfacial resistance is expressed as

$$\Phi_b{}' = \frac{1n\mu(4p^2 - \pi d^2)}{8} \frac{}{hp^2}\dot{L}^2\,LW \tag{S18}$$

The evolution of the dynamic spreading front is again expressed as

$$L_{ii} = \sqrt{\frac{8n\pi dh^2\gamma\cos\theta}{\mu\left[4h^2 f(\varphi_s) + n(4p^2 - \pi d^2)\right]}t} \tag{S19}$$

Therefore, the ratio of spreading speeds on WMPS (V_{ii}) and SMPS (V_i) can be concluded

$$\frac{V_{ii}}{V_i} = \frac{L_{ii}}{L_i} = \sqrt{1 + \frac{4(n-1)h^2 f(\varphi_s)}{4h^2 f(\varphi_s) + n(4p^2 - \pi d^2)}} \tag{S20}$$

Given the geometric constraint $p \geq d$, $n > 1$ and $f(\varphi_s) > 0$, our analysis proves

$$V_{ii} > V_i \tag{S21}$$

This fundamental analysis demonstrates that the engineered wrinkles on WMPS enhance the water spreading velocity compared to SMPS.

References

[1] J. Bico, C. Tordeux, D. Quere D. Rough wetting. *Europhys Lett.*, 2001, **55**, 214-220.

[2] W. Miao, S. Zheng, J. Zhou, B. Zhang, R. Fang, D. Hao, L. Sun, D. Wang, Z. Zhu, X. Jin, Y. Tian and L. Jiang, Microchannel and Nanofiber Array Morphology Enhanced Rapid Superspreading on Animals' Corneas, *Adv. Mater.*, 2021, **33**, 2007152.

[3] Sangani AS, Acrivos A. Slow flow past periodic arrays of cylinders with application to heat transfer. *Int. J. Multiphas. Flow*, 1982, **8**, 193-206.